Parallel Electron Temperature and Density Gradients measured in the JET MkI Divertor using Thermal Helium Beams

S. J. Davies, P. D. Morgan, Y. Ul'Haq[1], C. F. Maggi, S. K. Erents[2], W. Fundamenski[3], L. D. Horton, A. Loarte, G. F. Matthews, R. D. Monk and P. C. Stangeby[3]

JET Joint Undertaking, Abingdon, Oxon., OX14 3EA, UK.
[1] Imperial College of Science, Technology and Medicine, London, SW7 2BZ, UK.
[2] UKAEA Fusion, Culham, Abingdon, Oxon., OX14 3EA, UK.
[3] and Institute for Aerospace studies, University of Toronto, Canada.

ABSTRACT

This paper describes the first application of a thermal helium beam diagnostic to a divertor. The helium beam is used to determine spectroscopically the electron temperature and density from the inner and outer strike points up to the X-point, using helium line ratios which are primarily sensitive to electron density and temperature, as reported in [1]. Measurement of the neutral helium line intensities in the outer divertor target were performed under attached, high recycling and detached plasma conditions in Ohmic and L-mode discharges. An interpretative model has been developed using the DIVIMP code at JET which incorporates the helium injection point, the nozzle divergence and the viewing arrangement of the periscope for a particular equilibrium.

1. INTRODUCTION

Of fundamental importance to the understanding of divertor physics is the measurement of basic parameters such as the distribution of electron temperature and densities from the inner and outer strike points up to and beyond the X-point. These parameters are also needed in the validation of detachment models like, for example, EDGE2D [2]. In this paper the first application of a thermal helium beam diagnostic to a divertor capable of providing simultaneous measurements of the 2D distribution of electron density and temperature from the inner and outer strike points up to the X-point is described. Neutral helium line ratios which are primarily sensitive to electron density (667.82nm/728.13nm) and temperature (706.52nm/728.13nm) as reported in [1] are used. Data presented will concentrate on measurements performed in the outer divertor leg for Ohmic and L-Mode diverted discharges at various stages of detachment. Target electron densities and temperatures are provided from Langmuir probe measurements whilst electron temperatures for the inner divertor leg are provided by VUV spectroscopy measurements of the CII line ratio 90.41nm/133.53nm. These measurements provide some experimental validation of the helium beam derived electron temperatures.

The development of an interpretative model using the DIVertor IMPurity code DIVIMP [3] which generates the background hydrogenic plasma and incorporates diagnostic lines-of-sight utilising the JET atomic database ADAS [4] is also described. Such a model makes it easier to integrate experimental data with the modelling of detachment.

2. EXPERIMENTAL ARRANGEMENT

The arrangement of the helium injection nozzles and periscopes in the MkI divertor is shown in Figure 1. The nozzles and periscopes were situated in different sectors of the same octant such that any helium atom injected from one nozzle which became ionised was transported along the field lines away from the other nozzle. Target Langmuir probes were also situated in the same octant.

Helium was injected at a rate of 13 mbar litre/sec (~3×10^{20} He-atoms/sec) for typically two seconds with a thermal velocity of ~2×10^{3}m/s and the 'nozzle' used within the divertor was a 2mm ID 45mm long pipe with backing pressure ~200mbar. This was expected to give a divergence of ~40° FWHM [5]. The measurement of this divergence is currently being undertaken at IPP Berlin.

Each periscope consisted of ten 300μm all-silica fibres which covered a vertical distance of 60cm from the divertor floor. The fibres have a numerical aperture of 0.2 giving a 2.5cm diameter viewing cone at the helium injection points. A Spex 270M spectrometer with CCD camera, having a resolution of 1.3Å/pixel over a spectral range of 100nm at a 100ms sampling rate, was used to record the spectral intensities, an example of which is shown in Figure 2a. The background level of helium in the results shown here was negligible. If a large background level exists then it is possible to modulate, at up to 2Hz, the gas flow and to deconvolve the injected helium signal from the background recycling helium signal. Using a spectrometer to record simultaneously the neutral helium line intensities has certain advantages over using three independent CCD cameras with interference filters in that any time variations in sensitivities are reduced once a calibration has been done. In addition it is possible to account for the different background levels at each wavelength rather than assume a constant level.

Once the background level has been subtracted from each HeI line intensity, the two ratios are calculated and an example is shown in Figure 2b. Note that before the establishment of the helium flow from 13s onwards the fluctuation level in the ratios is large as a result of taking ratios of two small numbers. This noise level reduces significantly after 13s until after 19s, when the helium injection has stopped, when it begins to increase again. Electron densities and temperatures are calculated from these ratios using the atomic data and look up tables from the collisional-radiative model of [6]. In the future this step will be automated through collaboration with B. Schweer et al. at TEXTOR, KfA Jülich.

3. EXPERIMENTAL RESULTS

The neutral helium was injected from the private plasma region towards the separatrix where it was rapidly ionised. DIVIMP modelling of the neutral helium transport (of which more later) has shown that the photon emission at the wavelengths used is mainly from the separatrix. Consequently, thermal helium beam derived electron temperatures and densities given for the Ohmic and L-Mode examples below are quoted as the separatrix values. The strike points were swept at 4Hz and this sweeping is superimposed on the parallel electron density and temperature profiles shown below.

3.1 Ohmic Density Ramp Pulse 35430

During this Ohmic pulse the central line-averaged density was ramped from 2 to 6 $\times 10^{19}m^{-3}$ and the onset of high recycling at which the ion-flux to the inner and outer target began to decrease occurred at a central density of $3.5\times10^{19}m^{-3}$, after which the inner target became detached whilst the outer target became partially detached. Figure 3 shows the evolution of the electron temperature and density from the outer target, measured by Langmuir probes, up to the X-point as measured by the thermal helium beam diagnostic. The upstream electron temperature is first seen to be higher than, then reduces to become comparable to, the target temperature which is suggestive of a 'detachment front' propagating up to the X-point consistent with bolometer measurements on similar detached pulses [7].

At the inner target the Langmuir probe derived electron temperature was 5eV with the density peaking at $3\times10^{19}m^{-3}$ before steadily decreasing to $\sim10^{18}m^{-3}$ as the inner divertor leg became detached. VUV measurements of the CII emission from the inner divertor leg inferred that the electron temperature decreased from 8eV with low recycling to 3.5eV with high recycling and detachment. The target electron temperature derived from Langmuir probe measurements may be overestimated under high recycling and detached conditions as the sheath resistance begins to have a dominant effect upon the IV characteristic and a virtual double probe fitting routine has to be employed. Further details on this subject are given in [8].

The expected upstream temperatures calculated using the two-point model [9] were compared with those determined from the helium beam data and it was found that before the onset of detachment the agreement between the calculated and measured electron temperatures was generally good. With high recycling leading to detachment the two-point model calculations become invalid as no account is taken of parallel momentum losses through charge exchange. Consequently a large difference between the expected and observed temperatures occurred that was first seen at 2.2m along the field line and then further up towards the X-point.

Better agreement between modelled and measured electron temperatures was obtained with EDGE2D modelling [10] of the detachment as indicated in Table 1 below.

Outer Divertor conditions	EDGE2D (measured) Upstream Te (eV) at 2.2m	4.1m	8.1m along field line.
Low recycling	30 (25)	35 (30)	39 (40)
High recycling	10 (8.5)	14 (15)	26 (25)
Partial detachment	3 (4.5)	5.5 (6)	11 (15)

Table 1 : Comparison of EDGE2D calculated and measured electron temperatures at different distances along the outer divertor leg in Ohmic pulse 35430.

3.2 L-Mode Detachment Pulse 35390

In this 3.8MW neutral beam injected pulse the density was increased to $4.8\times10^{19}m^{-3}$ at 13s after which it remained constant up to 19s. Neutral helium was injected over this time period and the resulting parallel electron density and temperature variation is illustrated as a function of time in Figure 4. As previously the target electron densities and temperatures are provided from Langmuir probe measurements. The influence that the 4Hz sweeping of the strike points has on the profiles is more clearly seen in this figure.

The temperature at the target decreased from 30eV at 13s to 7eV at 15s whilst at the X-point it decreased from 40eV to 17eV. The target density peaked at approximately $1\times10^{20}m^{-3}$ whilst at the X-point it increased from $0.87\times10^{19}m^{-3}$ to $1.5\times10^{19}m^{-3}$. Such a high divertor density means that other atomic processes, such as volume recombination, must be occurring. These are not taken into account in the collisional-radiative model of [6]. Consequently the helium derived densities are probably lower than the actual densities.

At the inner divertor target the electron temperature peaked at 20eV at 13s rapidly decreasing to 5eV from 14s onwards when the inner divertor became detached. Correspondingly the electron density peaked at $1.5\times10^{20}m^{-3}$ reducing to $\leq5\times10^{19}m^{-3}$. Figure 5 shows the VUV measurements of the CII emission in the inner divertor inferring that the electron temperature decreases from 4.5eV to 3.5eV. However, as the figure shows, the CII signals may not be coming from the same location along the inner divertor leg. Before 14s the CII signals are strongly sensitive to the 4Hz sweeping of the strike points, indicating that the CII emission predominantly comes from the vicinity of the strike point. After 14s this oscillation is much reduced, indicating that the CII emission has moved upwards some distance along the inner divertor leg and is now predominantly within the acceptance cone of the VUV spectrometer.

4. DEVELOPMENT OF AN INTERPRETATIVE MODEL USING DIVIMP

The injection of helium atoms into the MkI divertor plasma and the measurement of neutral helium line intensities of 706.52nm, 728.13nm and 667.82nm along diagnostic lines of sight have been simulated using DIVIMP, a Monte-Carlo impurity transport code [3]. Helium atoms are launched into a background hydrogenic plasma from a point source and the trajectory of each particle is calculated using the Monte-Carlo method. Toroidal symmetry is assumed and the particle motion is mapped onto a 2-D poloidal plane. The calculations for both the background plasma and the injected impurities are performed on a non-orthogonal grid generated from magnetic measurements for a specific time in a pulse.

4.1 Background Plasma

A 2-D hydrogenic plasma is calculated based upon a 1-D model using Langmuir probe measurements of electron temperature and the ion saturation current density as boundary conditions at the targets. Such a background plasma model is described as an Onion Skin Model (OSM) [11, 12], and is a mixture of both experiment and theory. For this paper the Ohmic pulse 35430 under high recycling conditions at 16s was simulated. In the SOL an allowance has been made for full heat convection, that is both thermal and kinetic, and the electron and ion temperatures have been allowed to evolve separately. Hydrogenic ionisation and excitation have been included which results in some electron cooling and some impurity radiation has also been assumed to give electron temperature and density gradients which match the experimental data. Pressure (static and kinetic: $P_T = nkT(1+M^2)$) changes throughout the SOL increasing away from the target due to charge-exchange momentum losses.

The private plasma has been treated separately from the SOL. A simple prescription was applied which essentially divided the region in two. In the first half of the private plasma the electron and ion temperatures were gradually increased to a maximum equal to twice their target values, while the density along each field line was kept constant at the target value. In the second region the electron and ion temperatures were kept constant at their maximum value while the density was gradually increased by a factor of two.

4.2 Diagnostic Simulations

Neutral helium was injected into the private plasma at a temperature of 0.07eV and at an angle of +10° from the Z-axis. The neutral particles had a cosine distribution, with a divergence of 40 ° FWHM. The helium atoms travel through the divertor plasma in straight lines in the direction of their launch angle until they are ionised or collide with the divertor walls. The ionised helium is swept along the field lines out of the periscope field of view and are no longer followed. No helium recycling from the injected source or from other wall sources has been considered in this simulation. Sweeping of the separatrix has also been ignored in this example. Future simulations will account for the sweeping by running cases with the same plasma background grid and, for each simulation, injecting the helium at different locations representative of the sweeping.

Each injected helium atom is followed and the excitations that each one undergoes as it moves through the plasma are calculated and registered. In this way the neutral helium density and the density of the various helium atom excitations are calculated from the accumulated statistics of several thousand launched particles. A post-processor is then run which applies photon efficiencies from the TEXTOR atomic database [6] within ADAS [4], to which DIVIMP is coupled, at each point on the grid. The radiation intensity for each spectroscopic line of interest is calculated with the assumption that the helium excited level populations are in instantaneous equilibrium with the ground level density. The experimental spectroscopic signals are simulated by integrating the calculated line intensities along the ten periscope lines of sight which also includes the effect of finite viewing angle in the poloidal plane. A measurement of the location of these lines of sight has been obtained using the in-vessel viewing system IVIS [13]. Each line intensity is then plotted as a function of periscope viewing angle.

4.3 Results

The initial results from simulations of the helium beam diagnostic have been valuable in interpreting experimental results. DIVIMP predicts the transport of helium atoms from the point of injection towards the X-point. The experimentally determined electron temperature and density gradients and absolute values were matched by the DIVIMP calculation along the separatrix. This suggests that the experimental helium line intensities peak along the separatrix. A 2-D line intensity plot from the code is shown in Figure 6a which clearly shows the peaking of line intensity along the separatrix. Injecting the helium at other angles, for example at -10°, gave similar results. The shape of each line intensity plot as a function of periscope viewing angle also compared well with the observed distribution as shown in Figure 6b.

The values of the calculated density sensitive ratios (667.82nm/728.13nm) for each line of sight generally agree well with the corresponding experimental values as shown in Table 2 below :

Fibre	**DIVIMP**	**Measured**	**DIVIMP**	**Measured**
	706.52nm / 728.13nm		**667.82nm / 728.13nm**	
3	9.8	9.3	6.6	5.9
4	20	6.7	5.4	4.1
5	15.4	6.1	6.8	4.6
6	10	5.6	6.0	5.0
8	10	4.2	4.2	4.4

Table 2 : Comparison of DIVIMP calculated HeI line ratios with experimentally recorded ratios.

Larger variance was observed between the predicted temperature sensitive ratios (706.52nm/728.13nm) and the corresponding experimental values. This is probably a consequence of the way in which the photon emissivity coefficients are calculated by ADAS. The density sensitive ratio includes only singlet transitions while the temperature sensitive ratio includes a triplet transition (706.52nm). The subroutine used by ADAS to calculate photon efficiencies for triplet transitions is not the same as that used for singlet transitions and appears to result in larger discrepancies between the experimental and calculated temperature sensitive ratios. Resolving this issue is currently the main priority in the development of this interpretative model. Future work with the code will also include the effect of various recycling sources, the inclusion of electron-ion recombination from an ionised state of helium and the effect of separatrix sweeping on the helium distribution.

5. CONCLUDING REMARKS

A thermal helium beam diagnostic has been successfully implemented in the JET MkI divertor with measurements performed in Ohmic and L-Mode discharges. These measurements provide data essential for the understanding of divertor physics and experimental validation of the distribution of electron densities and temperatures calculated from detachment models such as EDGE2D. Modelled electron temperatures have obtained good agreement with the measured temperatures. The helium beam measured electron density probably represents a lower estimate under high density conditions. Future work will concentrate on taking into account other atomic processes such as volume recombination which become significant at these high densities. An interpretative model using the DIVIMP Monte-Carlo code which can, for example, deal with the beam divergence, has been and will continue to be developed. At present there appears to be a discrepancy in the ADAS database with respect to [6] for the triplet HeI line 706.52nm.

In the MkIIa divertor there is an additional injection point from the outer divertor side which is viewed spectroscopically from above. Other activities include the development of de Laval nozzles in collaboration with the Rutherford Appleton Laboratory, UK to obtain a more collimated helium beam.

6. REFERENCES

[1] Schweer, B. et al., J. Nucl. Mat. **196-198**, 174 (1992)

[2] Loarte, A., these Proceedings

[3] Stangeby, P. C. & Elder, J. D., 'A Guide to the DIVIMP Code', (1995)

[4] Summers, H. P., JET-IR(94) 06 (1994)

[5] Burrell, K., Rev. Sci. Instrum., **49**, 948 (1978)

[6] Brosda, B., PhD thesis, Rühr-Universitat, Bochum (1993)

[7] Reichle, R. et al., in Proc. 22nd EPS Conf. on Contr. Fus. Plas. Phys., **19C**, III-085(1995)
[8] Monk, R. D. et al., these Proceedings
[9] Keilhacker, M. et al., Physica Scripta, **T2/2**, 443 (1982)
[10] Loarte, A. et al., in preparation
[11] Erents, S. K. et al., these Proceedings
[12] Monk, R. D. et al., J. Nucl. Mat., **220-222**, 612 (1995)
[13] Raimondi, T. et al., 14th SOFT, France (1986)

ACKNOWLEDGEMENTS

The authors would like to acknowledge P. Andrew, T. Budd, Th. Hartrampf, J. How, H. Jensen, N. Lam, P. Prior, C. Walker, C. Wilson and M. Wykes for their invaluable assistance in the implementation of the thermal helium beam diagnostic at JET following the original proposal by G. F. Matthews, G. McCracken (currently at MIT), P. D. Morgan, B. Schweer (KfA Jülich), P. C. Stangeby and H. P. Summers.

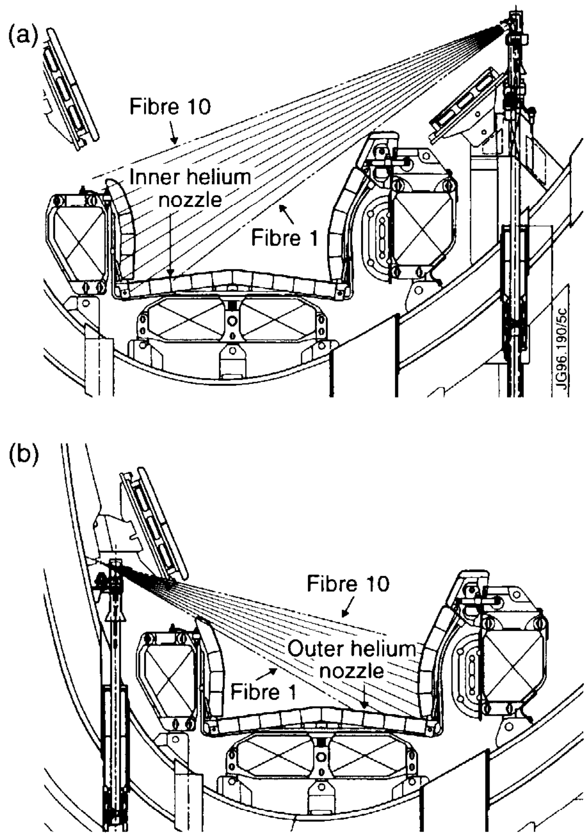

Figure 1 : Viewing arrangement for the thermal helium beam diagnostic in the JET MkI divertor for (a) Inner nozzle (Octant 5 Sector B) and (b) Outer nozzle (Octant 5 Sector C).

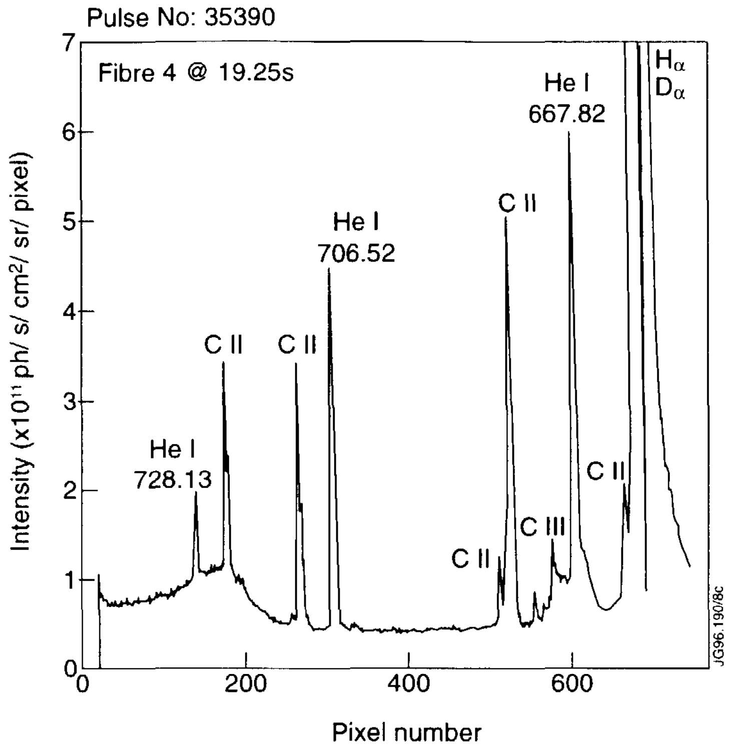

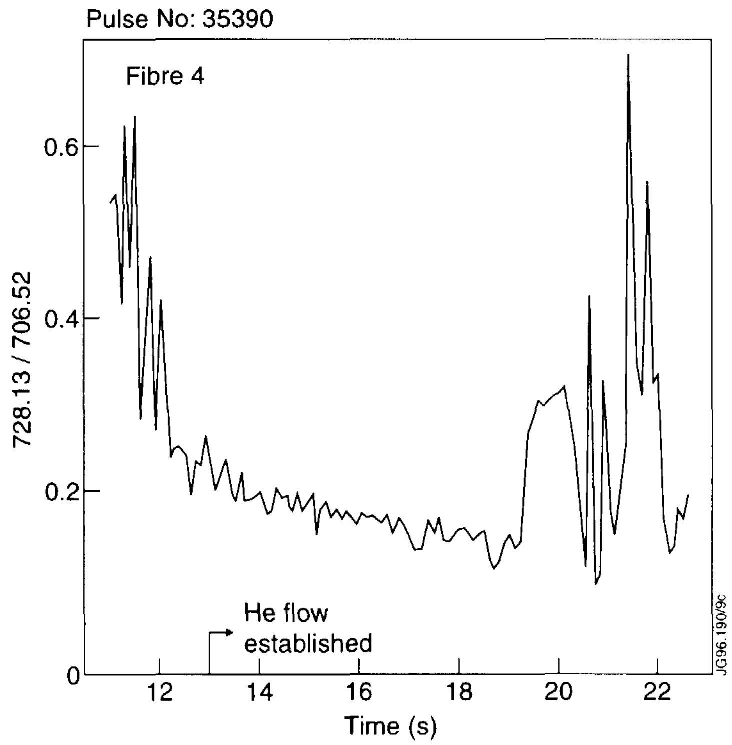

Figure 2 : (a) Example spectra recorded using Fibre 4 in Outer viewing periscope during L-Mode pulse 35390 and (b) resulting evolution of helium line ratio 728.13nm/706.52nm.

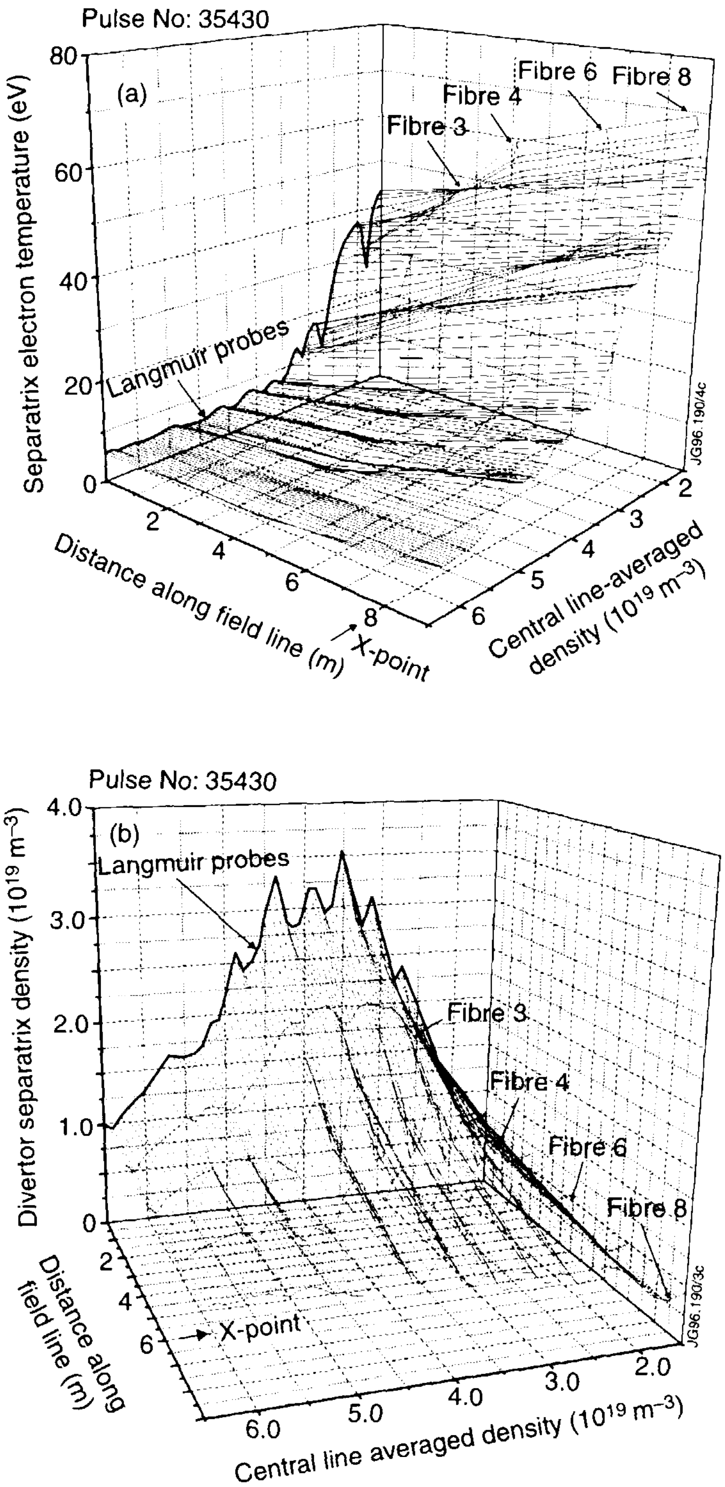

Figure 3: Spatial variation of (a) electron temperature and (b) electron density in outer divertor leg as a function of line-averaged density for ohmic pulse 35430.

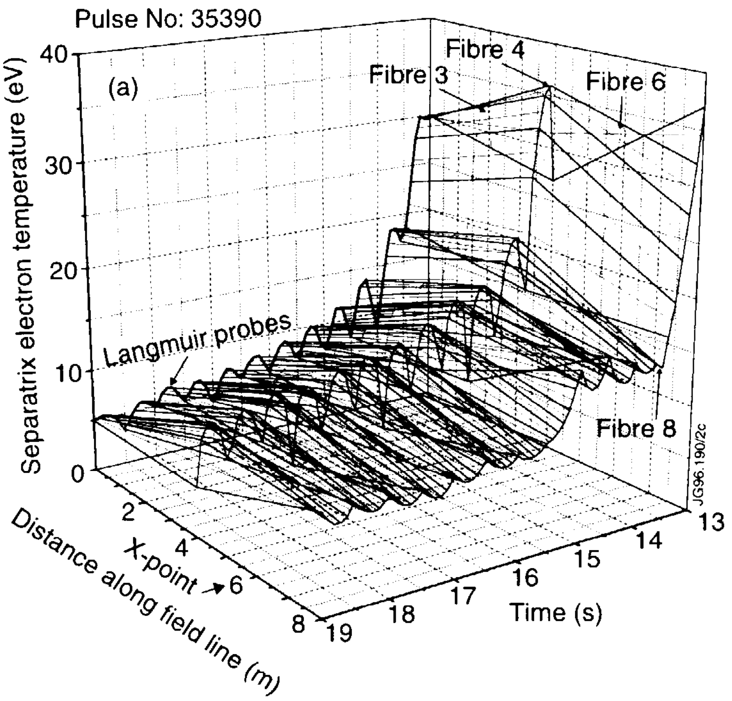

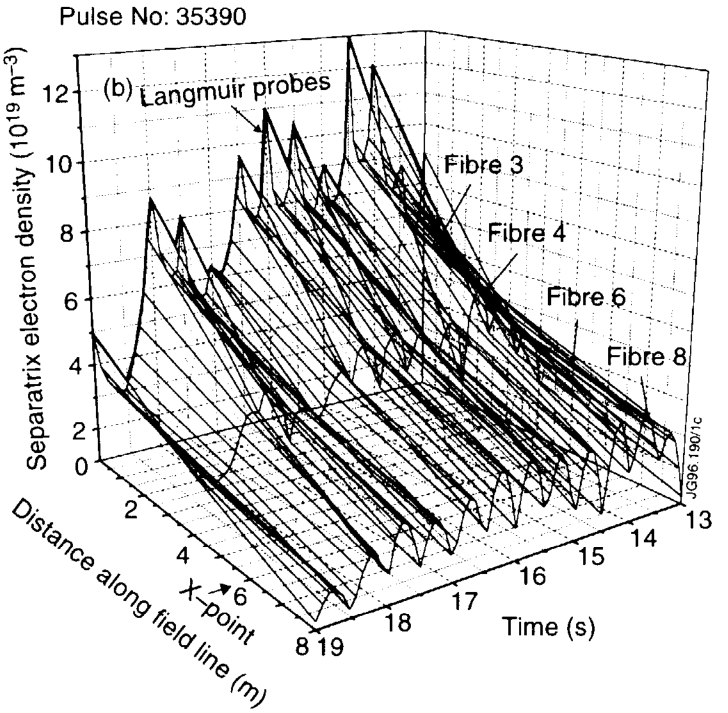

Figure 4: Spatial variation of (a) electron temperature and (b) electron density in outer divertor leg as a function of time in pulse 35390.

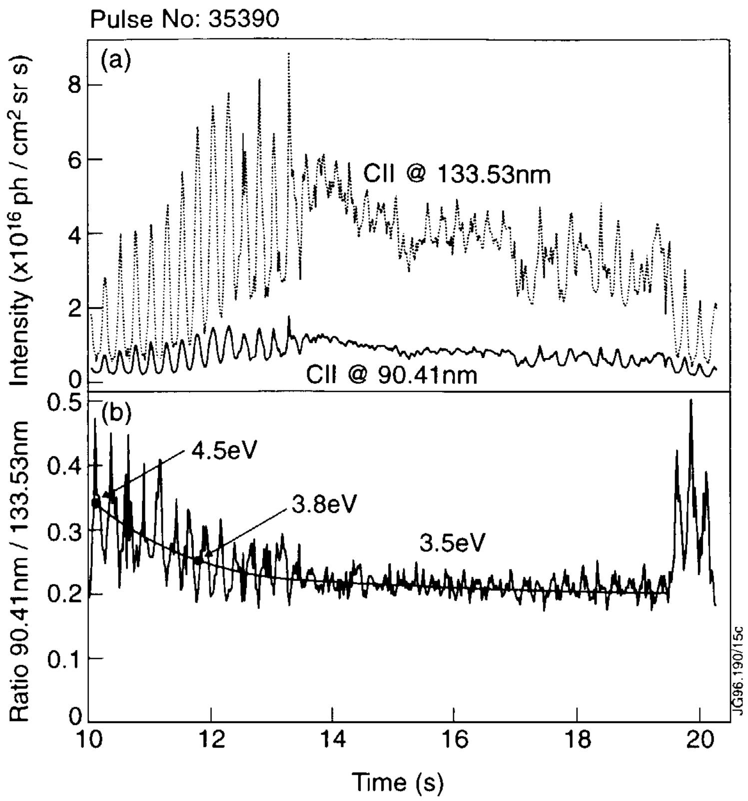

Figure 5: (a) Variation in CII lines 90.41nm and 133.53nm in inner divertor leg as measured by VUV spectroscopy with (b) consequent ratio and calculated electron temperature.

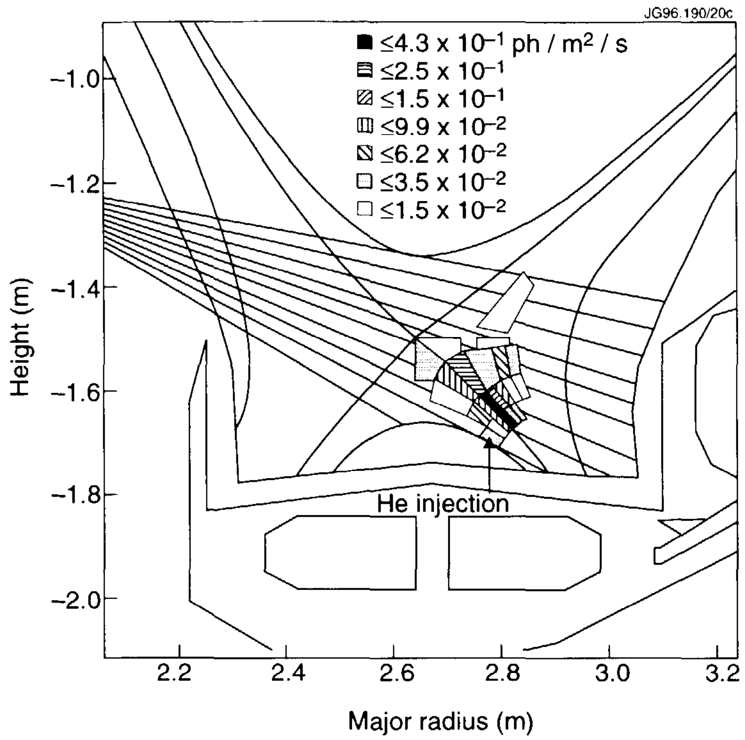

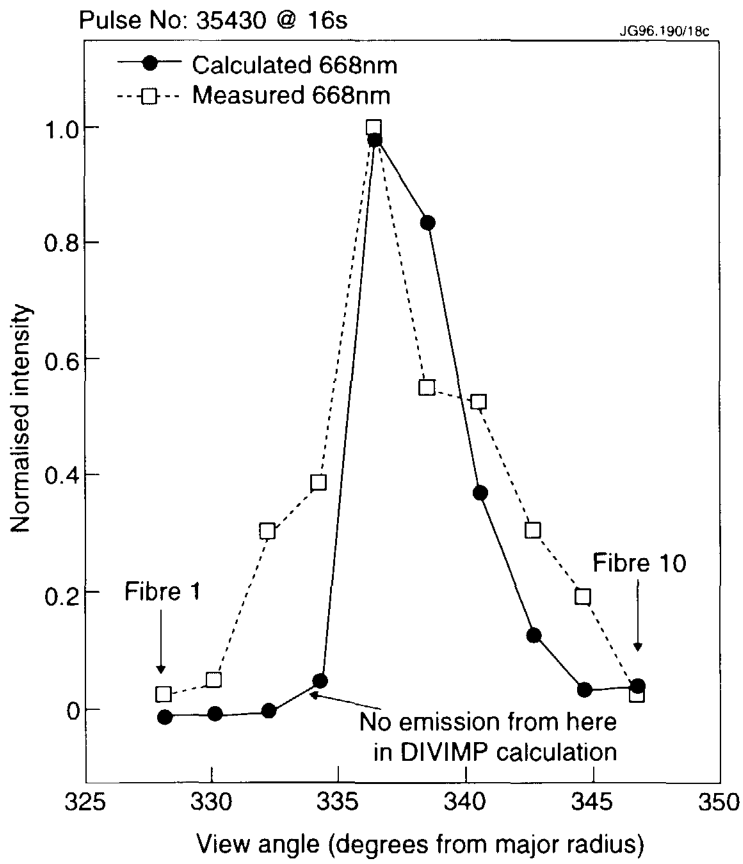

Figure 6 : (a) DIVIMP predicted spatial distribution of HeI line intensity at 728.13nm for Ohmic pulse 35430 under high recycling conditions at 16s and (b) normalised comparison of DIVIMP predicted and measured HeI (667.82nm) line intensities as a function of viewing angle/fibre.